Am J Cancer Res 2020;10(9):2832-2850
www.ajcr.us /ISSN:2156-6976/ajcr0116194

Original Article

SLFN5 influences proliferation and apoptosis by upregulating PTEN transcription via ZEB1 and inhibits the purine metabolic pathway in breast cancer

Xuefeng Gu[1,2,3*], Guoqing Wan[1,2,3*], Yue Yang[4*], Yihao Liu[5,6], Xintong Yang[2], Yanjun Zheng[1], Liying Jiang[2], Peng Zhang[7], Dingsheng Liu[1], Weiming Zhao[8], Gang Huang[2], Changlian Lu[2]

[1]Shanghai University of Medicine & Health Science Affiliated Zhoupu Hospital, Shanghai, P. R. China; [2]Shanghai Key Laboratory of Molecular Imaging, Shanghai University of Medicine & Health Sciences, Shanghai, P. R. China; [3]School of Pharmacy, Shanghai University of Medicine & Health Sciences, Shanghai, P. R. China; [4]Department of Pathology, Mudanjiang Medical University, Mudanjiang, P. R. China; [5]NHC Key Laboratory of Human Disease Comparative Medicine, Institute of Laboratory Animal Sciences, CAMS&PUMC, Beijing, P. R. China; [6]Beijing Engineering Research Center for Experimental Animal Models of Human Critical Diseases, Beijing, P. R. China; [7]School of Clinical Medicine, Shanghai University of Medicine & Health Sciences, Shanghai, P. R. China; [8]Qiqihar Medical University, Qiqihar, P. R. China. [*]Equal contributors.

Received June 12, 2020; Accepted August 14, 2020; Epub September 1, 2020; Published September 15, 2020

Abstract: Human Schlafen-5 (SLFN5) is aberrantly involved in tumorigenesis in several types of cancer. However, its implications in breast cancer (BRCA) are unknown. Herein, we demonstrated that SLFN5 expression is negatively associated with the tumour growth of human BRCA using GEO database analysis and clinical sample immunostaining. Lentiviral overexpression of SLFN5 in BRCA cell lines suppressed tumourigenicity in nude mice. Knockdown and overexpression of SLFN5 in BRCA cell lines proved that SLFN5 can inhibit cell proliferation and colony formation and promote apoptosis by upregulating the transcription of a known cancer suppressor gene (the phosphatase and tensin homologue on chromosome 10, PTEN), resulting in molecular changes in the downstream AKT pathway and in proliferation/apoptosis. Lentiviral knockdown and overexpression of ZEB1 blocked the changes in the PTEN and AKT pathways and in the colony formation ability caused by SLFN5 knockdown and overexpression, respectively. Luciferase reporter assays demonstrated that ZEB1 can inhibit the PTEN promoter activity in MCF7 cells by binding to a motif in the PTEN promoter. Metabonomics analysis showed that SLFN5 influences many metabolic pathways and especially decreases purine metabolites, including inosine, xanthine, and hypoxanthine. In conclusion, our findings suggest that SLFN5 may be an important protective factor against BRCA, as it regulates PTEN transcription, the AKT pathway, and proliferation/apoptosis via ZEB1 mediation and inhibits the purine metabolic pathway. Thus, SLFN5 may be a potential therapeutic target for BRCA.

Keywords: SLFN5, breast cancer, apoptosis, PTEN, purine metabolism

Introduction

Breast cancer (BRCA), a malignant tumour occurring in the epithelial tissue of the breast, is the most common cancer in women. BRCA screening has significantly reduced the mortality rate of BRCA since the development of early-stage cancer diagnosis technologies. However, BRCA still ranks as the second leading cause of cancer-related death worldwide. Annually, there are approximately 1.7 million new cases and more than 500,000 fatalities [1]. Elucidating the mechanism of BRCA tumourigenesis not only contributes to understanding the disease but also facilitates the development of new effective therapeutic targets to treat BRCA patients.

The Schlafen (SLFN) family was originally identified as a regulator of mouse thymocyte maturation and T cell activation [2]. Later, studies revealed that SLFN family members are involved in some basic cellular processes, including the control of viral replication, differentiation, and growth regulation [3, 4]. However, few studies on SLFN5 are available, and its role appears to

be cell type-dependent; SLFN5 negatively regulates mobility in renal carcinoma cells and malignant melanoma cells [5], while it promotes growth and invasion by inhibiting the transcription of the driving gene signal transducer and activator of transcription 1 (STAT1) in glioblastoma cells [6]. We recently found that SLNF5 plays an inhibitory role in migration and invasion by downregulating membrane type 1 matrix metalloproteinase (MT1-MMP) expression via AKT/GSK-3beta/beta-catenin in several types of cancer cells [7], and that SLFN5 can maintain and restore the epithelial morphology of BRCA cells by downregulating the transcription of ZEB1 [8]. However, the functions of SLFN5 in BRCA proliferation, apoptosis and metabolism are undetermined.

PTEN is considered a tumour suppressor gene that can dephosphorylate phosphatidylinositol-3, 4, 5-triphosphate (PIP3) to PIP2, thereby antagonizing phosphoinositide-3-kinase (PI3K) signalling and AKT phosphorylation/activation, which in turn affects cell cycle progression, apoptosis and motility [9-11]. In a variety of tumours, the PTEN protein is reduced or even absent due to genetic mutations or expression downregulation [12, 13]. In BRCA, the PTEN level is reduced; however, the mutation rate of the PTEN gene is approximately 5% [14], indicating that downregulation of PTEN expression may play a dominant role.

ZEB1 is a known transcription factor mainly involved in epithelial-to-mesenchymal transition (EMT) and metastasis in some cancers, including BRCA [15-18]. However, ZEB1 may play other roles in addition to its role in regulating morphological changes. As reported, approximately 2,000 genes are regulated by ZEB1, suggesting that ZEB1 may be involved in a central switch that controls cellular functions [19, 20]. Notably, knockdown of ZEB1 led to induction of PTEN with loss of constitutive pS473Akt [21]. We recently found that human SLFN5 can inhibit ZEB1 transcription by directly binding to the SLFN5 binding motif on the ZEB1 promoter, thereby maintaining the epithelial cell morphology and inhibiting metastasis in BRCA. However, whether SLFN5-regulated ZEB1 expression is involved in PTEN regulation and its related function in BRCA are undetermined.

With the deepening of tumour biology research, research on the role of cell metabolism abnormalities in tumour development has become an active international academic frontier [22-24]. Studying metabolic changes in tumours will provide important theoretical guidance for the molecular diagnosis of and targeted therapy for tumours. However, to date, the influence of SLFN5 on cancer metabolism is undetermined.

In this study, we analysed the role of SLFN5 in BRCA progression using the GEO database and human tissues. The effect of SLFN5 on the proliferation, colony formation and apoptosis of BRCA cells was explored *in vitro*. The effect of SLFN5 on BRCA tumour growth was verified *in vivo*. The regulatory mechanism of SLFN5 on PTEN transcription via ZEB1 and the downstream AKT pathway were explored. Finally, we studied the influence of SLFN5 on the metabolism of BRCA cells using metabonomic analysis.

Materials and methods

Cell culture and transfection

Human BRCA cell lines (MCF-7 and MDA-MB-231) were cultured as previously described [8]. Cells were cultured at 37°C in a humidified 5% CO_2 atmosphere and transfected using lentiviruses according to the manufacturer's specifications.

Preparation of recombinant lentiviruses

Recombinant overexpression vectors and shRNA vectors of SLFN5 and ZEB1 were cloned as described previously [8]. Briefly, SLFN5 (NM_44975.3) and ZEB1 (NM_001128128.2) full-length coding sequences were cloned into the lentiviral vectors GV358 and pLVX-IRES-NEO, respectively, and each empty vector served as a transfection control. Human SLFN5-specific shRNA and ZEB1-specific shRNA were introduced into the lentiviral vector, and scrambled shRNA was constructed as a negative control. Lentiviral particles containing SLFN5 and SLFN5-specific shRNA were transfected into MDA-MB-231 and MCF-7 cells, respectively, and selected with puromycin. All stably transfected cell lines were verified by detection of GFP fluorescence and SLFN5 protein expression. To study the role of ZEB1 in SLFN5-regulated proliferation and apoptosis, lentiviral particles containing ZEB1 were transfected into MDA-MB-231 cell lines stably expressing SLFN5, and lentiviral particles containing ZEB1-

specific shRNA were transfected into MCF7 cell lines stably silencing SLFN5.

Western blot analysis

Western blotting was performed as described previously [25]. Total protein was extracted from cells using RIPA lysis buffer (Thermo Fisher Scientific, Waltham, MA). Nucleus and cytosol proteins were separated using isolation kits (Beyotime Biotechnology, Shanghai, China). The protein concentrations were examined using a BCA Protein Quantification Kit (Yeasen, Shanghai, China). Proteins were separated on SDS-PAGE gels and transferred onto nitrocellulose membranes (Millipore, Bedford, MA, USA). The membranes were blocked with solution containing 5% non-fat dry milk and then incubated overnight at 4°C with specific primary antibodies, which included anti-SLFN5 from Sigma-Aldrich (Cat #HAP017760), and the following antibodies from Cell signalling technology, anti-PTEN (Cat #9188S), anti-Phospho-AKT (S473) (Cat #4060S), anti-Phospho-GSK-3β (Cat #9331), anti-Caspase-3 (Cat #9665S), anti-Cleaved Caspase-3 (Cat #9579S), anti-β-Catenin (Cat #8480), anti-Cyclin D1 (Cat #2922S), anti-Bax (Cat #2772S) and anti-β-actin (Cat #4967). The secondary antibodies, anti-rabbit or anti-mouse antibodies were obtained from Beyotime (Shanghai, China). After the membranes were washed, the blots were developed using an ECL kit (Yeasen, Shanghai, China).

Real-time PCR

Real-time PCR was performed as described previously [8]. Total RNA was extracted from lentiviral-infected MCF-7 and MDA-MB-231 cells using TRIzol® reagent (Invitrogen; Thermo Fisher Scientific, Inc.). According to the manufacturer's protocol, the total RNA was reversed transcribed into cDNA using the PrimeScript™ RT reagent kit (Takara Biotechnology Co., Ltd.), and qPCR was performed using the SYBR® Premix Ex Taq™ (Takara Biotechnology Co., Ltd.). Primers for PTEN were employed (sense 5'-TTGTGGTCTGCCAGCTAAA-3'; antisense 5'-CGCTCTATACTGCAAATGCT-3'), as were 18S rRNA-F primers (sense 5'-CCTGGATACCGCAGCTAGGA-3'; antisense 5'-GCGGCGCAATACGAATGCCCC-3') as a reference. The 2-ΔΔCt method was used to analyze relative changes in gene expression.

Immunohistochemistry

Immunohistochemistry was performed as previously described [26, 27]. In brief, breast carcinoma and corresponding pericarcinomatous tissues were frozen. The sections were fixed in ice-cold acetone for 0.5 h, washed in PBS, blocked for 1 h in PBS supplemented with Triton X-100 and normal serum, and then incubated with SLFN5 antibody (1:500; Sigma-Aldrich), at 4°C overnight. Finally, the sections were washed and incubated with secondary antibody for 1 h, followed by staining with DAB reagent. Breast carcinoma tissue samples and pericarcinomatous tissue samples used for immunohistochemical analysis were obtained from Harbin Medical University. All individuals who donated tissues for this study gave their consent in written form. All treatments and experimental protocols for this study were performed in accordance with established guidelines and regulations by the Biological and Medical Ethics Committee of Shanghai University of Medicine and Health Sciences. The Biological and Medical Ethics Committee of Shanghai University of Medicine and Health Sciences gave approval for the animal experiments.

Immunofluorescence

MCF-7 and MDA-MB-231 cells were cultured in a 12-well plate and transfected with lentiviruses for 24 h. MCF-7 cells were fixed with 4% paraformaldehyde for 15 min, permeabilized with 0.1% Triton-100, and blocked with 15% FBS for 1.5 h. Fixed MCF-7 cells were washed with PBS and incubated overnight at 4°C with an anti-Ki67 antibody (1:250; CST, Danvers, MA). After washing, MCF-7 cells were incubated with a fluorescence-conjugated secondary antibody (Jackson) for 2 h, and nuclei were stained with 4',6-diamidino-2-phenylindole (Roche) for 5 min. Ki67 was detected using a fluorescence microscope (EU5888; Leica, Germany).

Colony formation assay

For the colony formation assay, cells (500 per well) were seeded in a 6-well plate at 24 h post-transfection and cultured in medium containing 10% FBS for 10 days. When the colonies reached more than 50 cells, the colonies were fixed with 10% formaldehyde for 15 min and stained with 8.0% crystal violet for 10 min, followed by imaging using a digital camera. Each experiment was repeated three times.

Table 1. Associations of SLFN5 expression with clinicopathological parameters in breast cancer

Variables	Number	Mean (SLFN5)	*P* value		
Age					
Age>60	499	8.12±9.07			
Age≤60	618	8.71±8.29	0.260		
Sex					
Male	12	3.20±3.18			
Female	1106	8.50±8.67	7e-6[a]		
Menopause status					
Peri	41	10.56±10.48			
Post	720	8.22±8.31	0.214		
Pre	232	9.35±9.52	0.528	0.074	
Invasion of tumour					
T_1	284	9.38±10.1			
T_2	650	8.56±8.55	0.500		
T_3	141	6.59±5.93	4e-4	0.001	
T_4	40	6.83±5.65	0.020	0.076	0.816
Lymph node metastasis					
N_0	528	8.91±9.50			
N_1	371	8.22±8.42	0.251		
N_2	120	8.26±7.13	0.401	0.956	
N_3	79	7.66±6.12	0.123	0.497	0.529
pTNM-Stage					
Stage I	185	9.67±11.1			
Stage II	636	8.58±8.72	0.216		
Stage III	253	7.37±6.38	0.012[#]	0.024[#]	
Stage IV	20	5.02± 4.00	2.9e-4[#]	0.001[#]	0.023[#]
ER_status					
Negative	243	10.3±10.6	0.002[b]		
Positive	825	7.95±7.98			
PR_status					
Negative	350	9.25±9.96	0.060		
Positive	715	8.09±7.99			
Her2_status					
Negative	574	8.08±7.36	0.008[c]		
Positive	165	10.5±11.00			

P-values were calculated by a t-test. a, Male *vs* Female; b, ER-negative *vs* ER-positive; c, Her2-negative *vs* Her2-positive; #, refer to **Figure 1B**. Abbreviations: ER, oestrogen receptor; PR, progesterone receptor.

Flow cytometry assay

MCF-7 and MDA-MB-231 cells were seeded in 6-well plates at a density of 2×10^5 cells/well, cultured overnight, and then transfected with lentivirus or vector for 48 h. Then, the cells were harvested by trypsin, washed with ice-cold PBS twice, collected, fixed and stained using an Annexin V-APC/PI double-fluorescence apoptosis detection kit according to the manufacturer's instructions. The samples were then analysed by flow cytometry (BD FACS Calibur System; BD, USA).

TUNEL assay

DNA fragmentation was performed using a One-Step TUNEL Kit (Beyotime Biotechnology, Shanghai) following the manufacturer's recommendations. Briefly, MCF-7 and MDA-MB-231 cells were transfected and then fixed in 4% paraformaldehyde for 10 min at room temperature. Subsequently, the cells were washed with PBS three times and permeabilized for 2 min on ice, and the cells were resuspended in the TUNEL working solution. Following incubation for 1 h in a humidified atmosphere at 37°C in the dark, the cells were counterstained with a DAPI staining solution for 5 min at room temperature, and then, TUNEL-positive cells were visualized under a fluorescence microscope. DAPI was used for nuclear staining.

Tumourigenesis assay

Female nude athymic mice (7 weeks old, weighing approximately 18 g) were purchased from Shanghai Sippr BK Laboratory Animals, Ltd. Mice were maintained in a specific pathogen-free (SPF) animal facility. All animals received humane treatment according to the National Research Council's guidelines. MDA-MB-231 cells infected with lentiviruses were suspended at a final concentration of 5×10^7 cells/mL in PBS. A 100 μL aliquot of the cell suspension (approximately 5×10^6 MDA-MB-231 cells) was injected into the axilla region of the nude mice in the treatment group and the corresponding control mice. Mice were sacri-

Table 2. Primers for cloning the PTEN promoter fragment sequence into pGL-3

Name	Sequence
PTEN-1KpnIF2:	5'cggggtaccCAGCCCAATCGGGGCTGTAAACAGACTTGACAGGTTTGTT 3'
PTEN-2KpnIF:	5'cggggtaccGAGGCGGGGGCACGTGTTTGGATG 3'
PTEN-3KpnIF:	5'cggggtaccCCTGCGGGGTGCGTCCCACTCACAG 3'
PTENHindIIIR2:	5'cccaagcttGCAGGGCAGGGCAGGGGGCGGTAGGAGGGGGCAGAGCGGT 3'

ficed 28 days post-injection, and tumour growth was examined in these models. The tumour sizes and volumes were determined through external measurements and calculated by the formula: $V = [L \times W^2] \times 0.52$ (V = volume, L = length and W = width). The data were analysed using Student's *t*-test, and the differences were considered significant at $P < 0.05$.

Untargeted metabolomics analysis

To explore the potential presence between the SLFN5 knockdown and control groups, we developed and applied an untargeted metabolomics approach. For the metabolomics study, an equal number of cells (5×10^5 per mL) were seeded in P35 culture dishes. In all experiments, cells were plated at 90% confluence and completely attached to the plates. Nine replicates (cells cultured in different culture dishes) for each treatment were used. Chromatographic grade methanol, pyridine and chloroform were purchased from Merck Chemicals, and L-2-chlorophenylalanine was purchased from Sigma-Aldrich (St. Louis, MO, USA). An aliquot of 100 µL serum, 300 µL methanol-chloroform (3:1, v/v) solvent, 10 µL L-2-chlorophenylalanine (internal standard, 0.3 mg/mL in water) and C-17 (internal standard, 0.01 mg/mL in water) were mixed for metabolite extraction and then kept at -20°C for 10-20 min. After centrifugation at 13000 *g* for 20 min, 1 mL of supernatant was obtained and dried completely under nitrogen. Then, 250 µL methanol-water (7:3, v/v) was added as a solvent, and the solution was filtered with 0.22 µm microfilters. All extracellular media were collected and stored at -80°C for further analysis. Detailed parameters and data processing are described online in the Supplementary Materials and Methods.

Targeted metabolomics analysis

The appropriate amount of standard sample was weighed precisely by an analytical balance and dissolved in methanol to obtain the standard reserve solution. The standard sample information is shown in Table S1. A mixed standard solution was prepared from the above standard sample with gradient dilutions of 100 µg/mL, 50 µg/mL, 20 µg/mL, 10 µg/mL, 5 µg/mL, 2 µg/mL and 1 µg/mL. These were put into 1.5-mL Eppendorf (EP) tubes, and 100-µL gradient concentration mixtures and solvent were added into derivative vials before placing the vials in a rapid centrifugal dryer for derivative treatment. Detailed gas chromatography-mass spectrometry parameters are described in the Supplementary Material and Methods.

The appropriate standard (as shown in Table S2) was accurately weighed with the analytical balance, dissolved into a stock solution with a concentration of 1 mg/mL with methanol, and then serially diluted to a concentration of 100 µg/mL (working solution 1) or 1 µg/mL (working solution 2); working solution 1 was formulated into a mixed standard solution and then serially diluted to concentrations of 1000 ng/mL, 500 ng/mL, 200 ng/mL, 100 ng/mL, 50 ng/mL, 20 ng/mL, 10 ng/mL, 5 ng/mL, 2 ng/mL, and 1 ng/mL; working solution 2 was used for optimization of mass spectrometry conditions. Detailed ultra-performance liquid chromatography tandem mass spectrometry methods with electrospray ionization (UHPLC-ESI-MS/MS) parameters are described in the Supplementary Material and Methods (as shown in Table S3).

PTEN gene promoter activity analysis

The human PTEN promoter and the indicated length upstream from the transcription start site (TSS) were amplified from the MCF7 genome by qPCR and then cloned into the pGL-3 basic vector (Promega). The primers used for vector cloning are listed in **Table 2**.

These recombinant vectors were named PTEN-1 (-2000 bp~325 bp), PTEN-2 (-1500 bp~325 bp), PTEN-3 (-1060 bp~325 bp) and PTEN-4 (-478 bp~325 bp). The complete wild-type sequence of PTEN-3, 5'-GGGCACGTGTT-3' (-1053

to -1042 upstream from TSS) mutated to 5'-AAATGTACACC-3' and was named mutPTEN3-1. Similarly, mutPTEN3-2 refers to the mutation of the wild-type PTEN3 sequence from 5'-TGTGTACAGTT-3' (-826 to -815 upstream from TSS) to 5'-CTAGGTGGT-3'. mutPTEN3-3 refers to the mutation of the wild-type PTEN3 sequence from 5'-TGCAAGAAG-3' (-588 to -579 upstream of the TSS) to 5'-CTAGGTGGT-3'. mutPTEN3-4 refers to the mutation of the wild-type PTEN3 sequence from 5'-CAGGAGAGG-3' (-488 to -480 upstream from the TSS) to 5'-TCAACACAA-3'. Constructs were transfected into MCF7 cells overexpressing ZEB1 for luciferase activity assays. According to the manufacturer's instructions, firefly and Renilla luciferase activities were detected using the Dual-Luciferase Reporter Assay System (Promega).

Chromatin immunoprecipitation (ChIP) assay

ChIP assay was performed according to the manufacturer's instructions (26156, Thermo). Firstly, MCF-7 cells were cross-linked with 1% formaldehyde for 10 min at 37°C and quenched in 1.5 mL 10 × glycine solutions. Then, cells were harvested and washed with PBS. The cells were lysed, and chromatin was sonicated into 200~1000 bp fragments, and sedimented. Immunoprecipitations were performed with 8 μl of ZEB1 antibody (Cat #70512S ,CST, Danvers, MA, USA) or 2 μg of IgG control (Cat #A7001, Beyotime Biotechnology, Shanghai, China) overnight at 4°C. Ten percent of chromatin prior to immunoprecipitation was used as the input control. The precipitated DNAs were subjected to PCR to amplify the ZEB1 binding sites. The primers used in ChIP assays were as follows: PTEN Ch-IP1 F: 5'-CGGGTTTTCACGGCGGCCAAG-3'; PTEN Ch-IP 1 R: 5'-GGGCCCAAAGGGCACCTATC-3'; PTEN Ch-IP NC F: 5'-CACTTTGGGAGGTGGAGGTG- 3'; PTEN Ch-IP NC R: 5'-GTGTTTAAGCAATTCTCCTGC-3'. PCR was performed as follows: 98°C for 5 min, 32 cycles of 98°C for 30 s, 60°C for 20 s, and 72°C for 20 s, and a final extension step at 72°C for 5 min. The amplified fragments were then resolved electrophoretically on a 1.2% (w/v) agarose gel.

Statistical methods

GraphPad Prism 6.0 software (GraphPad Software, CA, USA) was used for data analysis. Data are expressed as the mean ± standard deviation (SD). Student's *t*-test or one-way analysis of variance (ANOVA) followed by Dunnett's post hoc test was utilized to analyse the differences between the two groups. $P < 0.05$ was considered statistically significant.

Results

Downregulated SLFN5 is associated with the malignancy of BRCA

Our previous study found that SLFN5 is negatively correlated with metastasis in BRCA [8]; however, we wondered whether it plays roles in the growth of BRCA. To evaluate the role of SLFN5 in BRCA growth and progression, fragments per kilobase of transcript per million mapped reads (FPKM) expression matrices and clinical data of 9264 tumour samples and 741 normal samples were downloaded from GSM1536837 and GSM1697009 (this project contains a total of 24 kinds of tumours). After screening, the BRCA FPKM expression matrix from the comprehensive FPKM matrix including 1119 tumour samples and 113 normal samples was analysed. The FPKM data showed that the SLFN5 transcript level was significantly lower in BRCA tissues than in normal tissues (**Figure 1A**), consistent with our previous findings of SLFN5 RNA expression analysis using TCGA data [8]. Moreover, we analysed the relationships between SLFN5 expression and the clinicopathological characteristics of BRCA patients and found that SLFN5 expression was negatively associated with clinical TNM stage and T stage according to tumour size (**Table 1**; **Figure 1B**, **1C**), suggesting that in addition to involving metastasis, as we recently reported, SLFN5 may be involved in BRCA progression. To further verify the aberrant expression of SLFN5, SLFN5 protein expression in BRCA and paracancerous normal tissues was examined by IHC with an anti-SLFN5 antibody. Compared with the nuclei of adjacent normal breast cells, the nuclei of BRCA cells were large, and the karyoplasm proportion was out of balance, showing typical tumour morphology (**Figure 1D**). SLFN5 protein was highly expressed in the epithelial cells of normal breast ducts and lobules but decreased in the nuclei of tumour cells (**Figure 1D**). SLFN5 scores of IHC staining decreased with tumour growth (**Figure 1E**), consistent with the GSM results above.

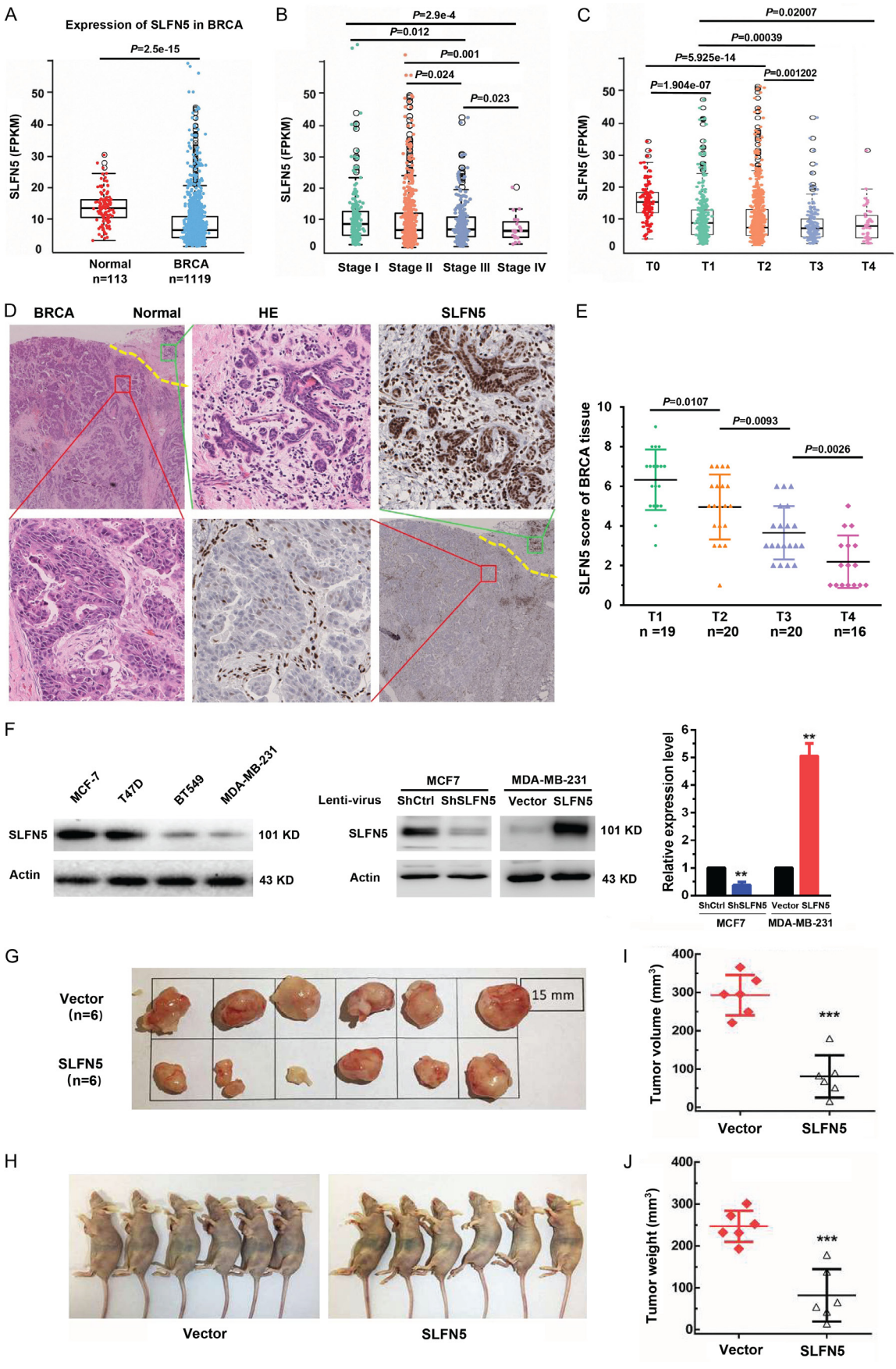
A
Expression of SLFN5 in BRCA
P=2.5e-15
SLFN5 (FPKM)
Normal n=113
BRCA n=1119
B
P=2.9e-4
P=0.012
P=0.001
P=0.024
P=0.023
SLFN5 (FPKM)
Stage I
Stage II
Stage III
Stage IV
C
P=0.02007
P=0.00039
P=5.925e-14
P=0.001202
P=1.904e-07
SLFN5 (FPKM)
T0
T1
T2
T3
T4
D
BRCA
Normal
HE
SLFN5
E
P=0.0107
P=0.0093
P=0.0026
SLFN5 score of BRCA tissue
T1 n =19
T2 n=20
T3 n=20
T4 n=16
F
MCF-7
T47D
BT549
MDA-MB-231
SLFN5
Actin
101 KD
43 KD
Lenti-virus
MCF7
MDA-MB-231
ShCtrl
ShSLFN5
Vector
SLFN5
Relative expression level
G
Vector (n=6)
SLFN5 (n=6)
15 mm
I
Tumor volume (mm3)
Vector
SLFN5
H
Vector
SLFN5
J
Tumor weight (mm3)
Vector
SLFN5

Figure 1. SLFN5 is downregulated in BRCA, and this downregulation is associated with tumour progression. A. The transcriptional level (FPKM value) of SLFN5 in BRCA and normal samples from the TCGA database. B. Correlation analysis was performed between the expression level of SLFN5 and clinical TNM stages. C. Correlation analysis was performed between the expression level of SLFN5 and primary tumour size. D. HE and SLFN5 immunohistochemical staining images of human adjacent normal tissues and BRCA tissues. E. Correlation analysis was performed between the immunohistochemical scores of SLFN5 and primary tumour size (n = 75). F. The protein levels of SLFN5 in the BRCA cell lines T47D, MDA-MB-231, MCF-7 and BT549. The protein levels of SLFN5 in MCF-7 cells with SLFN5 knockdown and in MDA-MB-231 cells with SLFN5 overexpression. G and H. SLFN5-overexpressing MDA-MB-231 cells were subcutaneously injected into nude mice, and representative tumour tissues were observed after 4 weeks. I. Tumour volumes were measured every four days. J. 28 days after implantation, the mice were euthanized, and the tumour nodules were weighed. HE & IHC, 100 × (black box), 400 × (blue box). $*P < 0.05$, $**P < 0.01$, $***P < 0.001$.

Next, a subcutaneous tumourigenesis experiment in nude mice was carried out to confirm the impact of SLFN5 on BRCA. We chose the BRCA cell line MDA-MB-231 with low SLFN5 expression for a functional study with a lentiviral transfection of SLFN5, and the overexpression of SLFN5 was confirmed by Western blot analysis (**Figure 1F**). MDA-MB-231 cells transfected with SLFN5-overexpressing lentiviruses or control lentiviruses were injected into the axillary region of female nude mice, and the tumour growth was monitored. The results indicate that overexpression of SLFN5 slowed the subcutaneous growth of MDA-MB-231 cells (**Figure 1G**, **1H**). After 28 days, the tumour volume and weight in the SLFN5-overexpressing group were both significantly decreased compared to those in the control group (**Figure 1I**, **1J**). Collectively, these results suggest that SLFN5 can inhibit the tumourigenicity of BRCA *in vivo*.

SLFN5 inhibits the proliferation and promotes the apoptosis of BRCA cells

To further detect whether SLFN5 can affect the growth of BRCA cells, BRCA cell line MCF-7 cells with high SLFN5 expression and MDA-MB-231 cells with low SLFN5 expression were transfected with lentiviruses of SLFN5-specific shRNA and overexpression vectors, respectively. Cell proliferation was detected using immunofluorescent staining of Ki67 in the nucleus. As shown in **Figure 2A**, knockdown of SLFN5 significantly facilitated the proliferation of MCF-7 cells, while overexpression of SLFN5 obviously reduced the proliferation of MDA-MB-231 cells. Next, a colony formation assay was performed to detect the foci formation ability of these cells. The colony formation ability was dramatically increased by SLFN5 knockdown but significantly suppressed by SLFN5 overexpression (**Figure 2B**). Colony formation could be influenced by proliferation and/or apoptosis, and we therefore continued to detect the effect of SLFN5 on BRCA cell apoptosis using flow cytometry and TUNEL assays. Compared with the control group, the SLFN5-knockdown group had significantly decreased apoptosis as shown by both flow cytometry and TUNEL assays (**Figure 2C-F**); however the SLFN5-overexpressing group had markedly increased apoptosis. We further examined the expression levels of some apoptosis-related proteins, such as Caspase-3 and Bax. Apoptosis is a protease cascade mediated by members of the caspase family. Caspase-3, the most critical downstream apoptotic executor, is cleaved and activated to lead to apoptosis. Bax is a key protein in triggering the apoptosis programme, which can open special channels for cytochrome C in the mitochondrial membrane, allowing cytochrome C to enter the cytoplasm. The results showed that the protein levels of cleaved caspase-3 and Bax were decreased by SLFN5 knockdown, while they were elevated by SLFN5 overexpression (**Figure 2G**). To date, for the first time, SLFN5 has been reported to have an apoptotic effect on cancer cells. Together, these results suggest that SLFN5 could inhibit proliferation and promote apoptosis, thereby acting as a suppressor gene in BRCA cells.

SLFN5 knockdown promotes upregulation of purine metabolic pathway metabolites in MCF-7 cells

To explore the mechanism by which SLFN5 regulates proliferation and apoptosis in BRCA cells, a nontargeted metabolomics analysis was used to assess the metabolic changes induced by silencing SLFN5 in MCF-7 cells. The stability of the analytical method used is a prerequisite for obtaining valid data. Therefore, we first used principal component analysis (PCA) to monitor and evaluate the method stability. The

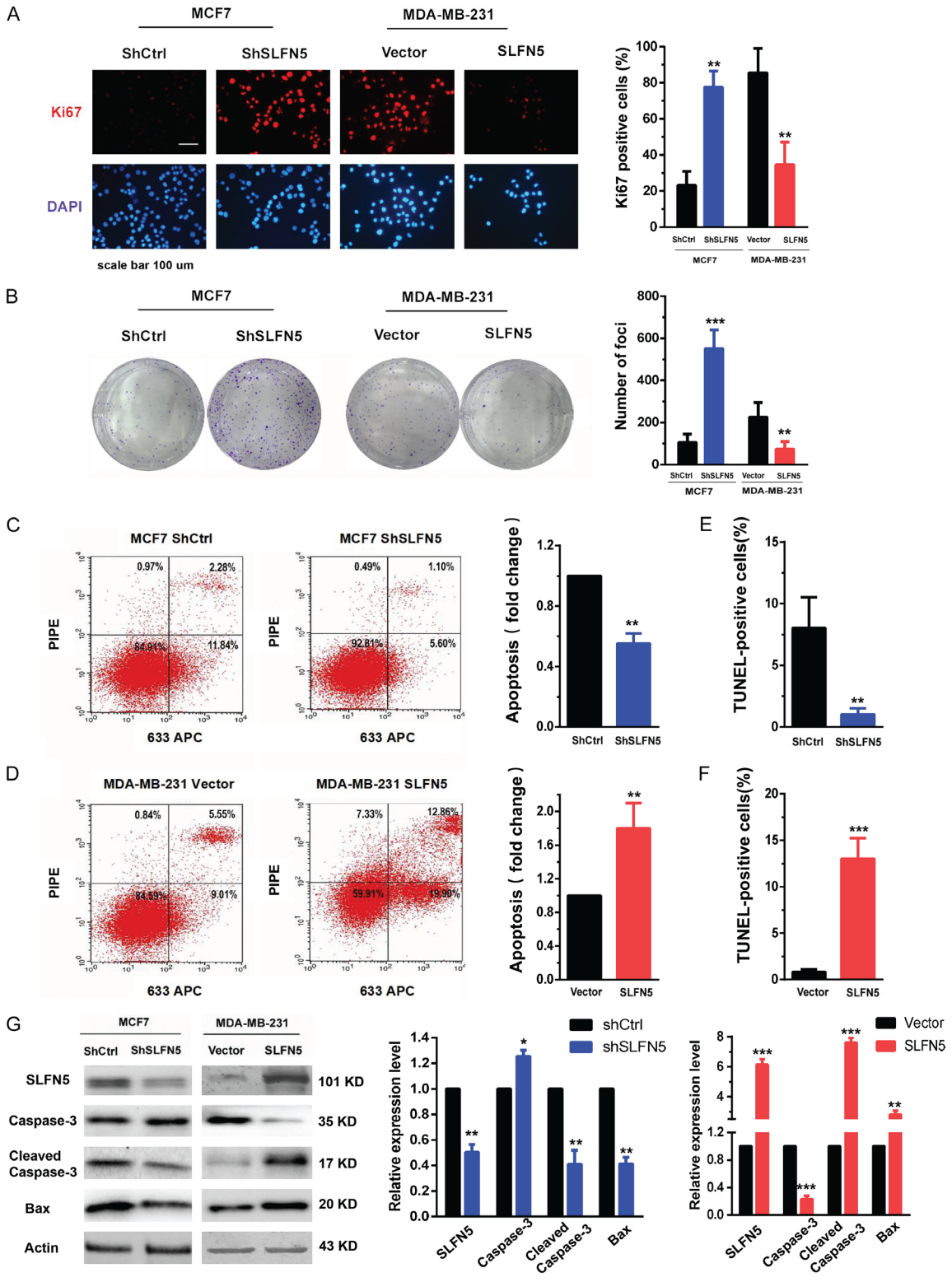

Figure 2. SLFN5 inhibits BRCA cell proliferation and promotes apoptosis. A. Proliferation analysis of BRCA cells with altered SLFN5 expression was performed by Ki67 immunofluorescence detection. B. Representative images of colony formation in BRCA cells with altered SLFN5 expression. C. Apoptosis analysis of MCF-7 cells with silenced SLFN5 expression was performed by flow cytometry. D. Apoptosis analysis of MDA-MB-231 cells overexpressing SLFN5 was performed by flow cytometry. E. Apoptosis analysis of MCF-7 cells with silenced SLFN5 expression was performed by a TUNEL assay. F. Apoptosis analysis of MDA-MB-231 cells overexpressing SLFN5 was performed by a

TUNEL assay. G. The expression of caspase-3, cleaved caspase-3 and Bax in BRCA cells with altered SLFN5 expression was determined using Western blotting. *$P < 0.05$, **$P < 0.01$, ***$P < 0.001$. Scale bar = 100 μm.

PCA model plot showed that the QC samples were tightly clustered, indicating that the analytical method was stable and reproducible (Figure S1A). Then, we utilized orthogonal partial least-squares discrimination analysis (OPLS-DA) to optimize the separation and access the metabolic difference between the SLFN5 knockdown and control groups. The model parameters for the variation R2Xcum (R2Xcum = 0.59), R2Ycum (R2Ycum = 0.59) and the predictive capability Q2cum (Q2cum = 0.78) were considerably high, which indicated that the model was suitable for data analysis (Figure S1B). Subsequent 7-fold cross validation and 200-response permutation testing (RPT) methods further strongly confirmed that the model was valid (Figure S1C). Pathway enrichment analysis of differential metabolites is helpful for understanding the mechanism of metabolic pathway changes in differential samples. Therefore, we used the KEGG database (http://www.genome.jp/KEGG/pathway.html) to obtain the enrichment results of the metabolic pathway. As shown in **Figure 3A** and **3B**, the intervention mechanism of SLFN5 in MCF-7 cells was mainly involved in pyrimidine metabolism, purine metabolism, glycolysis and arginine metabolism. We visualized the levels of metabolites involved in the above pathways that are significantly disrupted by SLFN5 in the heat map. The heatmap was plotted on a red-green colour scale, with red indicating an increase and green indicating a decrease in the metabolite levels. The results showed that the purine metabolite-related metabolites were significantly different between the groups, and the intragroup repeatability was good (**Figure 3C**). This result indicated that purine metabolism may be an important differentially regulated pathway in the progression of SLFN5-regulated BRCA.

Based on our previous nontargeted study results, for individual targeted validation of selected metabolites and quantification of the exact difference in purine pathway-related metabolites between the SLFN5 knockdown and control groups, a targeted metabolomics approach was performed with LC-MS or GC-MS. As shown in **Figure 3D**, after SLFN5 gene knockdown, the levels of inosine, adenine, hypoxanthine and xanthine in MCF-7 cells were upregulated compared with those in the control cells. The changes in marker metabolites in the purine metabolic pathway are summarized in **Figure 3E**. The fold changes in differentially regulated metabolites from nontargeted metabolomic analyses are indicated in black; fold change in differentially regulated metabolites from targeted metabolomics are indicated in yellow. These results further suggest that SLFN5 may regulate the purine metabolism pathway and participate in the tumourigenesis and development of BRCA.

SLFN5 inhibits the AKT signalling pathway in BRCA cells by upregulating PTEN expression

PTEN is a tumour suppressor gene. PTEN expression was decreased in BRCA with T stages (**Figure 4A**), consistent with the SLFN5 expression pattern in BRCA of GSM1536837 and GSM1697009 (**Figure 1A**). In our previous studies, we found that knockdown of SLFN5 can activate the AKT/GSK-3beta/beta-catenin pathway in MCF-7 cells, resulting in elevated migration and invasion; moreover, PTEN plays inhibitory roles in the AKT pathway, as has been reported in many studies. Therefore, is it possible that SLFN5 can affect PTEN expression? We found that SLFN5 knockdown significantly decreased PTEN expression, whereas SLFN5 overexpression significantly increased PTEN expression at both the mRNA and protein levels (**Figure 4B**, **4C**). Consistently, AKT pathway molecules, such as GSK-3beta, β-catenin and cyclin D1, negatively controlled by PTEN were activated or upregulated by SLFN5 knockdown in MCF-7 cells, whereas they were inactivated or downregulated by SLFN5 overexpression in MDA-MB-231 cells (**Figure 4D**). Furthermore, the specific inhibitor of PTEN, SF1670 (2.0 μM), was used to treat MDA-MB-231 cells with SLFN5 overexpression, and AKT phosphorylation were reversed (**Figure 4E**), suggesting that PTEN mediates SLFN5 functions in BRCA cell proliferation and apoptosis. Next, we explored whether SLFN5 regulates PTEN expression by binding to the PTEN promoter as a transcription factor. Checking our previous DNA sequencing data of chromosomal DNA fragments immunoprecipitated with the anti-SLFN5 antibody in MCF-7 cells, no marked binding peak of SLFN5 was found in the promoter region of *PTEN,*

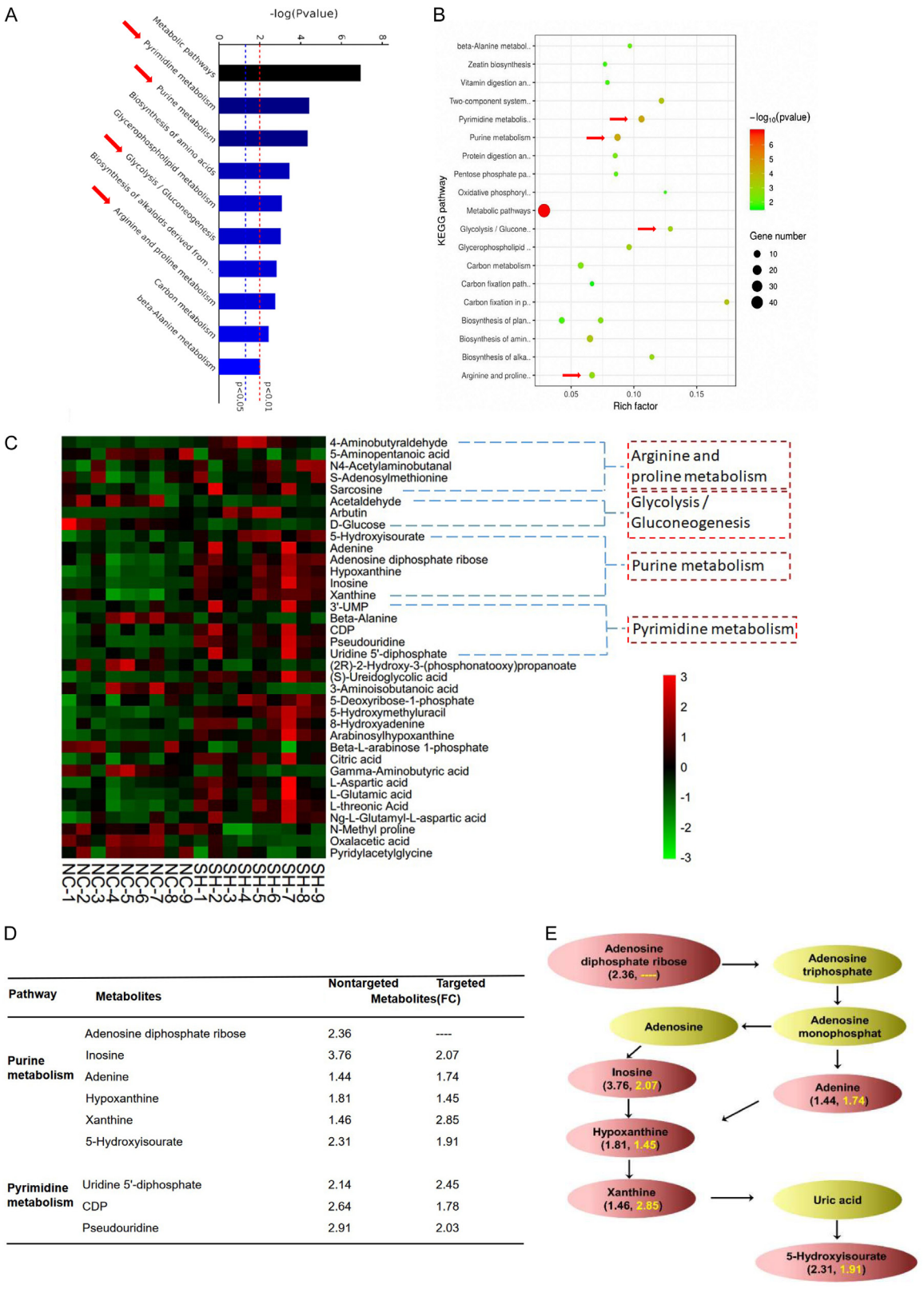

Pathway	Metabolites	Nontargeted Metabolites(FC)	Targeted Metabolites(FC)
Purine metabolism	Adenosine diphosphate ribose	2.36	----
	Inosine	3.76	2.07
	Adenine	1.44	1.74
	Hypoxanthine	1.81	1.45
	Xanthine	1.46	2.85
	5-Hydroxyisourate	2.31	1.91
Pyrimidine metabolism	Uridine 5'-diphosphate	2.14	2.45
	CDP	2.64	1.78
	Pseudouridine	2.91	2.03

Figure 3. Changes in the measured metabolites in MCF-7 cells with SLFN5 knockdown. A and B. The potential metabolic pathways of SLFN5 regulation in MCF-7 cells were analysed by KEGG analysis. Gene number is the number of metabolites of differentially regulated metabolites in the enriched metabolic pathway; rich factor is the ratio of differentially regulated metabolites to all metabolites in this pathway. C. Heat map of hierarchical clustering using intracellular metabolic data from MCF-7 cells with silenced SLFN5 expression and control cells. Red represents

upregulation, while green represents downregulation. D. Differentially regulated purine and pyrimidine metabolites derived from the nontargeted and targeted metabolomics analysis between the SLFN5 knockdown and control groups. E. Schematic representation of purine metabolite changes between the SLFN5 knockout group and the control group. Fold changes in differentially regulated metabolites from nontargeted metabolomics are indicated in black; fold changes in differentially regulated metabolites from targeted metabolomics are indicated in yellow.

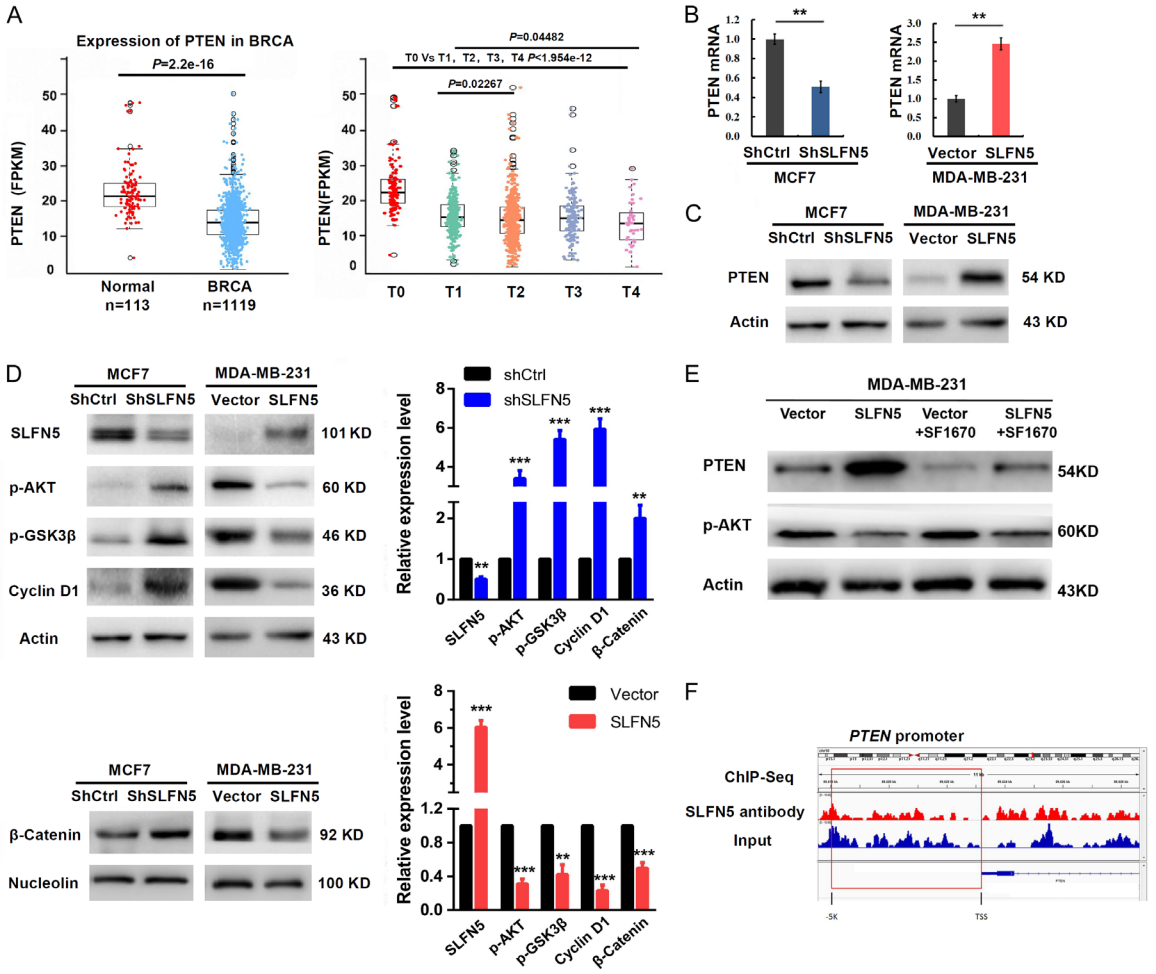

Figure 4. SLFN5 regulates the PTEN/AKT/cyclin D1 signalling cascades via ZEB1. A. TCGA analysis of PTEN expression in BRCA. B. The mRNA levels of PTEN in MCF-7 and MDA-MB-231 cells when SLFN5 was knocked down or overexpressed. C. The protein levels of PTEN in MCF-7 and MDA-MB-231 cells when SLFN5 was knocked down or overexpressed. D. Western blot analysis was used to determine the effect of SLFN5 knockdown or overexpression on proteins involved in the AKT signalling cascade in MCF-7 or MDA-MB-231 cells. E. Effect of SF1670 (2.0 μM) on MDA-MB-231 cells overexpressing SLFN5. F. The combination of SLFN5 and the PTEN promoter detected by ChIP-Seq. *$P < 0.05$, **$P < 0.01$, ***$P < 0.001$.

which is -5000 bp upstream of the TSS (**Figure 4F**). This suggests that the regulation of PTEN by SLFN5 could not result from direct binding of SLFN5 to the PTEN promoter as a transcriptional factor to act on PTEN transcription.

ZEB1 downregulates PTEN promoter activity in MCF7 cells

As reported by Liu *et al*. [21], knockdown of ZEB1 led to induction of PTEN and loss of constitutive pS473Akt. According to our recent studies, SLFN5 can directly bind to the ZEB1 promoter and inhibit ZEB1 transcription, and knockdown of SLFN5 can upregulate ZEB1 at both the mRNA and protein expression levels and vice versa (see our recently published EMT paper; **Figure 5A**). However, whether ZEB1 mediates SLFN5-directed PTEN expression needs to be explored. First, we silenced ZEB1 expression in MDA-MB-231 cells and found that the expression of PTEN was upregulated,

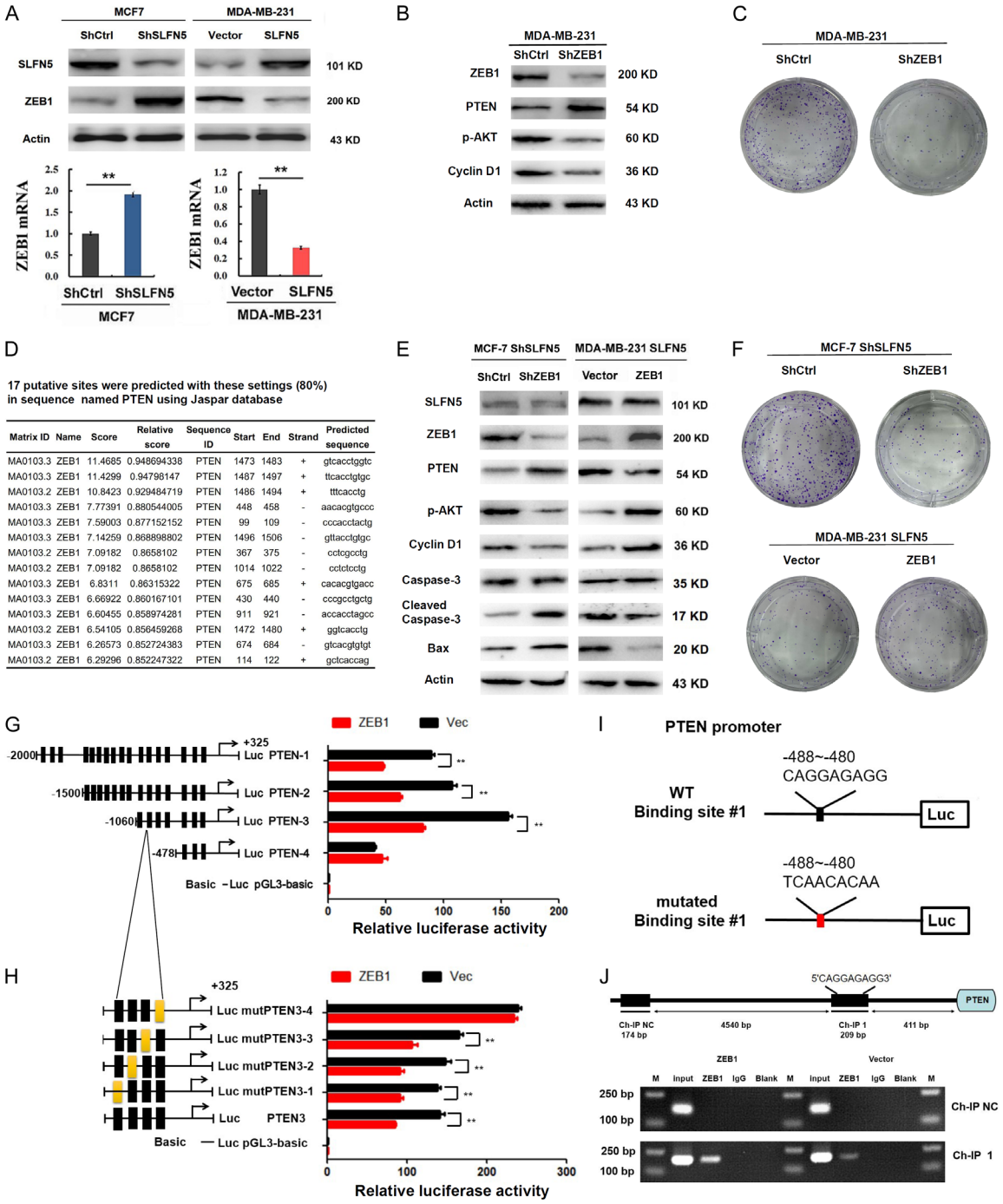

Figure 5. ZEB1 binds to the PTEN promoter and downregulates PTEN promoter activity in MCF7 cells. A. The protein levels of ZEB1 in MCF-7 and MDA-MB-231 cells when SLFN5 was knocked down or overexpressed. The mRNA levels of ZEB1 in MCF-7 and MDA-MB-231 cells when SLFN5 was knocked down or overexpressed. B. The effect of shZEB1 on MDA--MB-231 cells. C. The colony formation ability of MDA-MB-231 cells was reduced by shZEB1. D. Prediction of the binding sites of ZEB1 and PTEN promoter regions by Jaspar. E. The protein levels of SLFN5, ZEB1, PTEN, p-AKT, cyclin D1, caspase-3 and Bax in MCF7 or MDA-MB-231 cells when SLFN5 and ZEB1 were simultaneously knocked down or overexpressed. F. Representative images of colony formation in MCF7 or MDA-MB-231 cells when SLFN5 and ZEB1 were simultaneously knocked down or overexpressed. G. The relative activities of different regions of the PTEN promoter were examined by luciferase reporter gene assays in MCF7-NC and MCF7-ZEB1 cells. H. Relative luciferase activities of the PTEN promoter and mutants in MCF7 cells with and without ZEB1 overexpression. I. The key binding site of the PTEN promoter for ZEB1. J. ChIP assay revealed that ZEB1 binds to the PTEN promoter in MCF-7 cells. *P < 0.05, **P < 0.01.

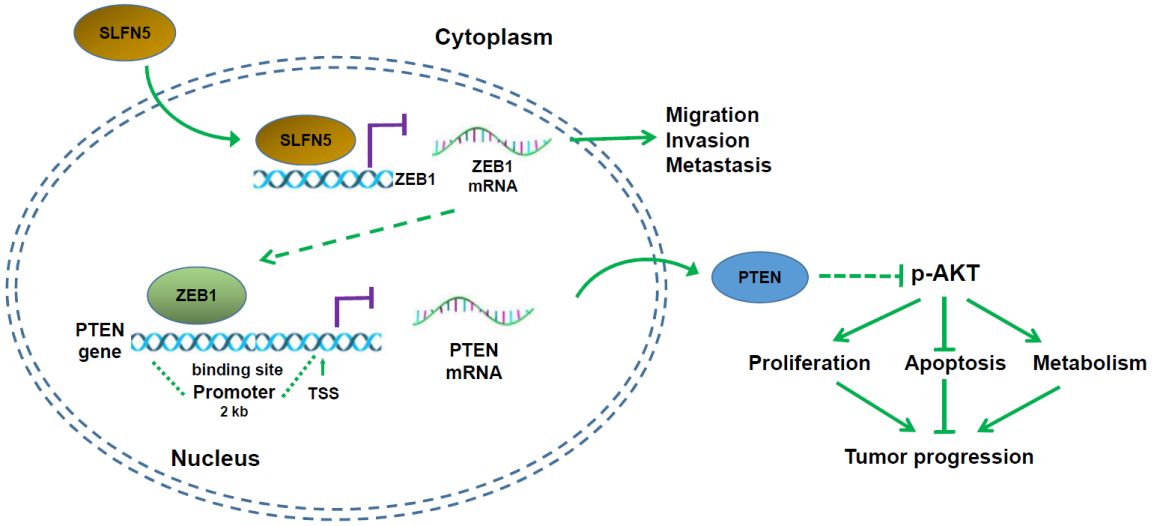

Figure 6. Schematic diagram of the mechanism by which SLFN5 regulates BRCA progression.

followed by the inhibition of the AKT pathway and colony formation (**Figure 5B**, **5C**). Then, we found that some binding sites of ZEB1 exsit regions according to the prediction of the Jaspar database (**Figure 5D**), that ZEB1 could mediate SLFN5-directed PTEN expression. To reverse this effect, knockdown of ZEB1 was performed in SLFN5-silenced MCF-7 cells. ZEB1 knockdown obviously reversed the protein levels of PTEN, p-AKT, cyclin D1, cleaved Caspase-3 and Bax resulting from SLFN5 knockdown (**Figure 5E**). Furthermore, forced ZEB1 expression in SLFN5-overexpressing MDA-MB-231 cells markedly reversed these protein expression levels resulting from SLFN5 (**Figure 5E**). It was also found that interfering with the expression of ZEB1 abolished the promoting effect of shSLFN5 on the colony formation ability of MCF7 cells, while the inhibition of SLFN5 overexpression was reversed by ZEB1 overexpression, and the effects on MDA-231 cell colony formation were reversed (**Figure 5F**). Therefore, these data suggest that SLFN5 regulates PTEN expression and modulates the apoptosis and proliferation of BRCA cells by mediating ZEB1.

To further determine whether ZEB1 could transcriptionally regulate *PTEN* expression, the luciferase activity of the PTEN promoter was determined in ZEB1-overexpressing MCF-7 cells. As shown in **Figure 5G**, PTEN-4 (-478 bp~325 bp), which had the shortest promoter region, was not influenced by ZEB1, but the other three promoters of PTEN, PTEN-1 (-2000 bp~325 bp), PTEN-2 (-1500 bp~325 bp) and PTEN-3 (-1060 bp~325 bp), were all decreased in the presence of ZEB1. Strikingly, PTEN-3 had the highest luciferase activity, indicating that this fragment of PTEN-3 (-1060 bp~-478 bp) includes the ZEB1-binding motif in the PTEN promoter. Together with the Jaspar database prediction results, the four binding motifs in this fragment were individually mutated, mutPTEN3-1 (-1053 bp~-1042 bp), mutPTEN3-2 (-826 bp~-815 bp), mutPTEN3-3 (-588 bp~-579 bp) and mutPTEN3-4 (-488 bp~-480 bp), and their promoter activities were determined. As shown in **Figure 5H**, the effects of ZEB1 inhibition on mutPTEN3-4 (-488 bp~-480 bp 5'-CAGGAGAGG-3' mutated to 5'-TCAACACAA-3') promoter activity almost disappeared compared with those on the vector control. This result indicated that ZEB1 could inhibit the activity of the PTEN promoter by binding to the 488 bp~480 bp fragment of the PTEN promoter (**Figure 5I**). Finally, a ChIP assays further demonstrated that ZEB1 directly binds to the promoter region (CAGGAGAGG) of PTEN in MCF-7 cells (**Figure 5J**).

To summarize, SLFN5 protein downregulation in BRCA cells increases the transcriptional activity of ZEB1; subsequently, upregulated ZEB1 protein further binds to the PTEN promoter, thereby inhibiting PTEN expression, activating the AKT pathway, and promoting the progression of BRCA (**Figure 6**).

Discussion

Tumours are new cell clusters that abnormally proliferate in the body. During the tumourigenesis process, some genes related to cell cycle regulation change to varying degrees, and the most important changes are those in some proto-oncogenes and tumour suppressor genes. Because the SLFN family plays an important role in cell proliferation and the immune response, researchers have explored the function of SLFNs in the field of tumours [28]. Studies have found that SLFNs are a group of genes involved in cell cycle progression and growth inhibition control, in which SLFN2 has a negative regulatory effect on malignant cell metastasis and growth [29], and SLFN1 plays an important role in inducing cell cycle arrest caused by DNA damage and cell apoptosis [30, 31]. As a new member of the SLFN family, SLFN5 has been found to be involved in several tumours in recent years [5-7, 32]. SLFN5 expression correlates with high-grade gliomas and shorter overall survival in patients suffering from glioblastoma multiform [6]. Elevated SLFN5 protein expression in patients with intestinal metaplasia correlates with progression to gastric cancer [32]. SLFN5 plays key roles in controlling the motility and invasiveness of renal cell carcinoma cells [5]. Our previous study found that SLFN5 expression negatively correlated with the aggressiveness of several cancer cells [7]. We recently found that SLFN5 inhibits metastasis by inhibiting ZEB1 transcription in BRCA. However, whether SLFN5 regulates BRCA tumourigenesis needs to be discerned.

In this study, we found that the expression of SLFN5 in BRCA was decreased, and that the SLFN5 expression level was negatively correlated with tumour size as well as tumour stage. The subcutaneous tumour formation experiment showed that overexpression of SLFN5 inhibited tumour growth in nude mice. Then, we altered SLFN5 expression in BRCA cell lines to evaluate the biological function of SLFN5 *in vitro*. SLFN5 overexpression significantly inhibits cell proliferation and promotes apoptosis. These results suggest that SLFN5 may act as a tumour suppressor gene to regulate the development of BRCA. Next, we found that SLFN5 increased PTEN protein expression, decreased p-AKT, p-GSK3β, β-catenin and cyclin D1 expression, and increased the protein levels of Bax and cleaved caspase-3 in BRCA cells. Considerable evidence indicates that the PTEN/PI3K/AKT pathway plays an important role in BRCA [33-35]. PTEN is considered to be another important tumour suppressor gene in addition to p53. Inactivation of PTEN leads to activation of the PI3K/AKT pathway, which can promote the growth, proliferation, invasion and metastasis of tumour cells and can inhibit apoptosis [36-40]. Glycogen synthase kinase 3β (GSK3β) is one of the downstream effector proteins of p-AKT. P-AKT inactivates GSK3β by phosphorylation, thereby inhibiting the degradation of cyclin D1 by GSK3β. Cyclin D1 is a key protein that regulates the G1 phase of the cell cycle, and cyclin D1 is a downstream target protein of active β-catenin, which plays an important role in promoting cancer cell proliferation [41]. Studies have found that p-AKT can decrease the activity of GSK3β by phosphorylation and prevent β-catenin phosphorylation and degradation; as a result, more β-catenin enters the nucleus and activates transcription of a series of cell proliferation- and differentiation-related target genes [42]. In addition to affecting proliferation, p-AKT can inhibit the apoptosis programme by upregulating the Bax protein levels on the mitochondrial membrane. Bax is responsible for opening the cytochrome C channel to release cytochrome C into the cytoplasm, where it forms apoptotic bodies with other molecules and causes a series of caspase cascade reactions. Caspase-3 is the final caspase molecule and is activated as cleaved caspase-3, which ultimately leads to cell apoptosis. Our results are consistent with the above findings, so we speculate that SLFN5 inhibits the AKT pathway by upregulating PTEN, leading to a decrease in cyclin D1 expression and an increase in the Bax levels, therefore inhibiting proliferation and promoting apoptosis in BRCA.

SLFN5 nuclear localization tends to support some transcriptional regulatory action. We found that SLFN5 can inhibit PTEN mRNA expression and that PTEN promoter activity was positively correlated with the SLFN5 levels. However, when we analysed previous ChIP-Seq data from SLFN5 antibody-immunoprecipitated chromosomal DNA, the results were unexpected: no marked binding peaks of SLFN5 were present in the promoter region of *PTEN*, sug-

gesting that SLFN5 could not direct *PTEN* transcription by binding to the PTEN promoter. In our recent studies on BRCA [8], we found that ZEB1 was a mediator of SLFN5-governed EMT, wherein SLFN5 can directly bind to the SLFN5 binding motif on the ZEB1 promoter, thereby inhibiting ZEB1 transcription. As reported by Liu *et al.* [21], knockdown of ZEB1 led to induction of PTEN with the loss of constitutive pS473Akt. Therefore, we further detected ZEB1 function in the process of SLFN5 regulation of PTEN expression. The results of both knockdown and overexpression of ZEB1 provided evidence that ZEB1 mediated the pathway by which SLFN5 regulates PTEN mRNA and protein expression and p-AKT activation, as well as proliferation and apoptosis. Furthermore, PTEN promoter luciferase reporter results proved that ZEB1 could suppress the transcriptional activity of the *PTEN* promoter, suggesting that ZEB1 mediates SLFN5 regulation of PTEN transcription.

Numerous studies have found that metabolic reprogramming of tumour cells and the understanding of tumour metabolism are no longer limited to changes in glycolysis and the tricarboxylic acid cycle; many metabolic pathways, including fatty acid metabolism, glutamine metabolism, serine metabolism, and choline metabolic changes, occur in tumour cells [43]. Cellular metabolic abnormalities have gradually become the target of tumour therapy in research [44, 45]. Metabolomics can be further divided into nontargeted and targeted metabolomics, depending on the purpose of the study. Nontargeted metabolomics is advantageous for identifying additional differentially regulated metabolites by focusing on the comprehensive analysis of metabolites in test samples [46]. However, targeted metabolomics is a more quantitative approach focused on a specific class of metabolites for in-depth study and analysis of subsequent metabolic molecular markers [47]. In our study, we obtained differentially expressed metabolites from MCF-7 cells transfected with sh-SLFN5 lentiviral particles and from control cells by nontargeted metabolomics analysis. Through metabolic pathway analysis, purine metabolism was found to possibly be the main metabolic pathway regulated by SLFN5. Subsequently, we further analysed the changes in key metabolites in the purine metabolic pathway through targeted metabolomics research, and the levels of inosine, adenosine, hypoxanthine and xanthine were significantly increased in cancer cells with SLFN5 knocked down.

The enhancement of purine metabolites supports RNA/protein synthesis, and transcriptional reprogramming is important for tumour cell proliferation [48]. Pedley AM et al. revealed that purine metabolites can provide cells with essential energy and cofactors to facilitate cell survival and propagation, thus fuelling cancer progression [49]. The purine metabolism pathway has been reported to be involved in the regulation of the occurrence and progression of BRCA. For example, Gunnar Schramm et al. revealed important features of 19 different pathways by analysing the metabolic pathways that regulate BRCA, including increased biosynthesis of purines, in 250 patient samples [50]. The antineoplastic drug methotrexate directly inhibits the de novo purine synthesis that occurs in MCF-7 BRCA cells [51]. Cao S et al. found that purine metabolites such as adenosine, guanosine, xanthine and xanthosine dihydrate increased in oestradiol-treated MCF-7 cells. This finding suggests that oestradiol could enhance purine metabolism to promote the development of BRCA [52]. In our present study, knockdown of SLFN5 increased purine metabolism, thereby promoting BRCA cell growth. The tumour metabolic changes observed in these studies will provide important theoretical guidance for precise diagnosis, prognosis and drug response analyses.

Conclusions

In the present work, we found that SLFN5 acts as a BRCA suppressor gene; regulates the proliferation, colony formation and apoptosis of MCF-7 and MDA-MB-231 cells; and inhibits tumour growth in nude mice. These regulatory effects are associated with changes in the PTEN/AKT pathway. Finally, metabolomic detection revealed that SLFN5 is involved in purine metabolic pathways in BRCA cells and regulates the levels of metabolites, including inosine, hypoxanthine, and xanthine. Based on the above research results, this study may provide new theoretical guidance for the molecular diagnosis of and targeted therapy for BRCA.

Acknowledgements

This work was supported by the National Natural Science Foundation of China (81772829

and 81830052), the Key projects for collaborative innovation of Shanghai University of Medicine & Health Sciences, Construction project of Shanghai Key Laboratory of Molecular Imaging (18DZ2260400), Shanghai Municipal Education Commission (Class II Plateau Disciplinary Construction Program for Medical Technology of SUMHS, 2018-2020), and the Funding Scheme for Training Young Teachers in Shanghai Colleges (ZZJKYX19009).

Disclosure of conflict of interest

None.

Address correspondence to: Changlian Lu and Gang Huang, Shanghai Key Laboratory of Molecular Imaging, Shanghai University of Medicine & Health Sciences, Shanghai 201318, P. R. China. Tel: +86-21-65883218; Fax: +86-21-65883218; E-mail: lvcl@sumhs.edu.cn (CLL); huangg@sumhs.edu.cn (GH); Weiming Zhao, Qiqihar Medical University, Qiqihar 161006, P. R. China. Tel: +86-452-2663311; Fax: +86-452-2663311; E-mail: zhaowm1969@126.com (WMZ)

References

[1] Ojo D, Rodriguez D, Wei F, Bane A and Tang D. Downregulation of CYB5D2 is associated with breast cancer progression. Sci Rep 2019; 9: 6624.

[2] Schwarz DA, Katayama CD and Hedrick SM. Schlafen, a New family of growth regulatory genes that affect thymocyte development. Immunity 1998; 9: 657-668.

[3] Puck A, Aigner R, Modak M, Cejka P, Blaas D and Stockl J. Expression and regulation of Schlafen (SLFN) family members in primary human monocytes, monocyte-derived dendritic cells and T cells. Results Immunol 2015; 5: 23-32.

[4] Katsoulidis E, Mavrommatis E, Woodard J, Shields MA, Sassano A, Carayol N, Sawicki KT, Munshi HG and Platanias LC. Role of interferon {alpha} (IFN{alpha})-inducible Schlafen-5 in regulation of anchorage-independent growth and invasion of malignant melanoma cells. J Biol Chem 2010; 285: 40333-40341.

[5] Sassano A, Mavrommatis E, Arslan AD, Kroczynska B, Beauchamp EM, Khuon S, Chew TL, Green KJ, Munshi HG, Verma AK and Platanias LC. Human Schlafen 5 (SLFN5) is a regulator of motility and invasiveness of renal cell carcinoma cells. Mol Cell Biol 2015; 35: 2684-2698.

[6] Arslan AD, Sassano A, Saleiro D, Lisowski P, Kosciuczuk EM, Fischietti M, Eckerdt F, Fish EN and Platanias LC. Human SLFN5 is a transcriptional co-repressor of STAT1-mediated interferon responses and promotes the malignant phenotype in glioblastoma. Oncogene 2017; 36: 6006-6019.

[7] Wan G, Liu Y, Zhu J, Guo L, Li C, Yang Y, Gu X, Deng LL and Lu C. SLFN5 suppresses cancer cell migration and invasion by inhibiting MT1-MMP expression via AKT/GSK-3beta/beta-catenin pathway. Cell Signal 2019; 59: 1-12.

[8] Wan G, Zhu J, Gu X, Yang Y, Liu Y, Wang Z, Zhao Y, Wu H, Huang G and Lu C. Human Schlafen 5 regulates reversible epithelial and mesenchymal transitions in breast cancer by suppression of ZEB1 transcription. Br J Cancer 2020; 123: 633-643.

[9] Wu J, Chen H, Ye M, Wang B, Zhang Y, Sheng J, Meng T and Chen H. Long noncoding RNA HCP5 contributes to cisplatin resistance in human triple-negative breast cancer via regulation of PTEN expression. Biomed Pharmacother 2019; 115: 108869.

[10] Gao C, Yuan X, Jiang Z, Gan D, Ding L, Sun Y, Zhou J, Xu L, Liu Y and Wang G. Regulation of AKT phosphorylation by GSK3β and PTEN to control chemoresistance in breast cancer. Breast Cancer Res Treat 2019; 176: 291-301.

[11] Papa A and Pandolfi PP. The PTEN(-)PI3K axis in cancer. Biomolecules 2019; 9: 153.

[12] Guo Y and Pei X. Tetrandrine-induced autophagy in MDA-MB-231 Triple-negative breast cancer cell through the inhibition of PI3K/AKT/mTOR signaling. Evid Based Complement Alternat Med 2019; 2019: 7517431.

[13] Milella M, Falcone I, Conciatori F, Cesta Incani U, Del Curatolo A, Inzerilli N, Nuzzo CM, Vaccaro V, Vari S, Cognetti F and Ciuffreda L. PTEN: multiple functions in human malignant tumors. Front Oncol 2015; 5: 24.

[14] Chai C, Wu H, Wang B, Eisenstat DD and Leng RP. MicroRNA-498 promotes proliferation and migration by targeting the tumor suppressor PTEN in breast cancer cells. Carcinogenesis 2018; 39: 1185-1196.

[15] Spaderna S, Schmalhofer O, Wahlbuhl M, Dimmler A, Bauer K, Sultan A, Hlubek F, Jung A, Strand D, Eger A, Kirchner T, Behrens J and Brabletz T. The transcriptional repressor ZEB1 promotes metastasis and loss of cell polarity in cancer. Cancer Res 2008; 68: 537-544.

[16] Eger A, Aigner K, Sonderegger S, Dampier B, Oehler S, Schreiber M, Berx G, Cano A, Beug H and Foisner R. DeltaEF1 is a transcriptional repressor of E-cadherin and regulates epithelial plasticity in breast cancer cells. Oncogene 2005; 24: 2375-2385.

[17] Krebs AM, Mitschke J, Lasierra Losada M, Schmalhofer O, Boerries M, Busch H, Boettcher M, Mougiakakos D, Reichardt W, Bronsert P, Brunton VG, Pilarsky C, Winkler TH, Brabletz S, Stemmler MP and Brabletz T. The EMT-activa-

tor Zeb1 is a key factor for cell plasticity and promotes metastasis in pancreatic cancer. Nat Cell Biol 2017; 19: 518-529.
[18] Larsen JE, Nathan V, Osborne JK, Farrow RK, Deb D, Sullivan JP, Dospoy PD, Augustyn A, Hight SK, Sato M, Girard L, Behrens C, Wistuba II, Gazdar AF, Hayward NK and Minna JD. ZEB1 drives epithelial-to-mesenchymal transition in lung cancer. J Clin Invest 2016; 126: 3219-3235.
[19] Caramel J, Ligier M and Puisieux A. Pleiotropic Roles for ZEB1 in cancer. Cancer Res 2018; 78: 30-35.
[20] Maturi V, Enroth S, Heldin CH and Moustakas A. Genome-wide binding of transcription factor ZEB1 in triple-negative breast cancer cells. J Cell Physiol 2018; 233: 7113-7127.
[21] Liu Y, Siles L, Lu X, Dean KC, Cuatrecasas M, Postigo A and Dean DC. Mitotic polarization of transcription factors during asymmetric division establishes fate of forming cancer cells. Nat Commun 2018; 9: 2424.
[22] Lu J. The Warburg metabolism fuels tumor metastasis. Cancer Metastasis Rev 2019; 38: 157-164.
[23] Levine AJ and Puzio-Kuter AM. The control of the metabolic switch in cancers by oncogenes and tumor suppressor genes. Science 2010; 330: 1340-1344.
[24] Kang H, Kim H, Lee S, Youn H and Youn B. Role of metabolic reprogramming in epithelial(-) mesenchymal transition (EMT). Int J Mol Sci 2019; 20: 2042.
[25] Ma T and Zhang J. Upregulation of FOXP4 in breast cancer promotes migration and invasion through facilitating EMT. Cancer Manag Res 2019; 11: 2783-2793.
[26] Saporiti F, Piacentini L, Alfieri V, Bono E, Ferrari F, Chiesa M and Colombo GI. Melanocortin-1 receptor positively regulates human artery endothelial cell migration. Cell Physiol Biochem 2019; 52: 1339-1360.
[27] Gu X, Wan G, Chen N, Li J, Chen B, Tang Y, Gu W, Jin C, Meng J, Zhang P, Liu L, Yang Z and Lu C. DGKzeta plays crucial roles in the proliferation and tumorigenicity of human glioblastoma. Int J Biol Sci 2019; 15: 1872-1881.
[28] Mavrommatis E, Arslan AD, Sassano A, Hua Y, Kroczynska B and Platanias LC. Expression and regulatory effects of murine Schlafen (Slfn) genes in malignant melanoma and renal cell carcinoma. J Biol Chem 2013; 288: 33006-33015.
[29] Katsoulidis E, Carayol N, Woodard J, Konieczna I, Majchrzak-Kita B, Jordan A, Sassano A, Eklund EA, Fish EN and Platanias LC. Role of Schlafen 2 (SLFN2) in the generation of interferon alpha-induced growth inhibitory responses. J Biol Chem 2009; 284: 25051-25064.
[30] Li M, Kao E, Malone D, Gao X, Wang JYJ and David M. DNA damage-induced cell death relies on SLFN11-dependent cleavage of distinct type II tRNAs. Nat Struct Mol Biol 2018; 25: 1047-1058.
[31] Zoppoli G, Regairaz M, Leo E, Reinhold WC, Varma S, Ballestrero A, Doroshow JH and Pommier Y. Putative DNA/RNA helicase Schlafen-11 (SLFN11) sensitizes cancer cells to DNA-damaging agents. Proc Natl Acad Sci U S A 2012; 109: 15030-15035.
[32] Companioni Napoles O, Tsao AC, Sanz-Anquela JM, Sala N, Bonet C, Pardo ML, Ding L, Simo O, Saqui-Salces M, Blanco VP, Gonzalez CA and Merchant JL. SCHLAFEN 5 expression correlates with intestinal metaplasia that progresses to gastric cancer. J Gastroenterol 2017; 52: 39-49.
[33] Liu C, Liu Z, Li X, Tang X, He J and Lu S. MicroRNA-1297 contributes to tumor growth of human breast cancer by targeting PTEN/PI3K/AKT signaling. Oncol Rep 2017; 38: 2435-2443.
[34] Sun D, Lei W, Hou X, Li H and Ni W. PUF60 accelerates the progression of breast cancer through downregulation of PTEN expression. Cancer Manag Res 2019; 11: 821-830.
[35] Wang L, Yang C, Liu XB, Wang L and Kang FB. B7-H4 overexpression contributes to poor prognosis and drug-resistance in triple-negative breast cancer. Cancer Cell Int 2018; 18: 100.
[36] Bazzichetto C, Conciatori F, Pallocca M, Falcone I, Fanciulli M, Cognetti F, Milella M and Ciuffreda L. PTEN as a prognostic/predictive biomarker in cancer: an unfulfilled promise? Cancers (Basel) 2019; 11: 435.
[37] Han K, Li C, Zhang X and Shang L. DUXAP10 inhibition attenuates the proliferation and metastasis of hepatocellular carcinoma cells by regulation of the Wnt/beta-catenin and PI3K/Akt signaling pathways. Biosci Rep 2019; 39: BSR20181457.
[38] Shi J, Liu Z and Xu Q. Tumor necrosis factor receptor-associated factor 6 contributes to malignant behavior of human cancers through promoting AKT ubiquitination and phosphorylation. Cancer Sci 2019; 110: 1909-1920.
[39] Cheng SY, Chen NF, Lin PY, Su JH, Chen BH, Kuo HM, Sung CS, Sung PJ, Wen ZH and Chen WF. Anti-Invasion and Antiangiogenic Effects of Stellettin B through Inhibition of the Akt/Girdin Signaling Pathway and VEGF in glioblastoma cells. Cancers (Basel) 2019; 11: 220.
[40] Duan HX, Li BW, Zhuang X, Wang LT, Cao Q, Tan LH, Qu GF and Xiao S. TCF21 inhibits tumor-associated angiogenesis and suppresses the growth of cholangiocarcinoma by targeting

PI3K/Akt and ERK signaling. Am J Physiol Gastrointest Liver Physiol 2019; 316: G763-G773.
[41] Liu SL, Liu Z, Zhang LD, Zhu HQ, Guo JH, Zhao M, Wu YL, Liu F and Gao FH. GSK3beta-dependent cyclin D1 and cyclin E1 degradation is indispensable for NVP-BEZ235 induced G0/G1 arrest in neuroblastoma cells. Cell Cycle 2017; 16: 2386-2395.
[42] Zhao Y, Song K, Zhang Y, Xu H, Zhang X, Wang L, Fan C, Jiang G and Wang E. TMEM17 promotes malignant progression of breast cancer via AKT/GSK3beta signaling. Cancer Manag Res 2018; 10: 2419-2428.
[43] Carvalho TM, Cardoso HJ, Figueira MI, Vaz CV and Socorro S. The peculiarities of cancer cell metabolism: a route to metastasization and a target for therapy. Eur J Med Chem 2019; 171: 343-363.
[44] Li X, Wenes M, Romero P, Huang SC, Fendt SM and Ho PC. Navigating metabolic pathways to enhance antitumour immunity and immunotherapy. Nat Rev Clin Oncol 2019; 16: 425-441.
[45] O'Sullivan D, Sanin DE, Pearce EJ and Pearce EL. Metabolic interventions in the immune response to cancer. Nat Rev Immunol 2019; 19: 324-335.
[46] Yumba Mpanga A, Siluk D, Jacyna J, Szerkus O, Wawrzyniak R, Markuszewski M, Matuszewski M, Kaliszan R and Markuszewski MJ. Targeted metabolomics in bladder cancer: from analytical methods development and validation towards application to clinical samples. Anal Chim Acta 2018; 1037: 188-199.
[47] Zhang X, Zhu X, Wang C, Zhang H and Cai Z. Non-targeted and targeted metabolomics approaches to diagnosing lung cancer and predicting patient prognosis. Oncotarget 2016; 7: 63437-63448.
[48] Teruya T, Chaleckis R, Takada J, Yanagida M and Kondoh H. Diverse metabolic reactions activated during 58-hr fasting are revealed by non-targeted metabolomic analysis of human blood. Sci Rep 2019; 9: 854.
[49] Pedley AM and Benkovic SJ. A new view into the regulation of purine metabolism: the purinosome. Trends Biochem Sci 2017; 42: 141-154.
[50] Schramm G, Surmann EM, Wiesberg S, Oswald M, Reinelt G, Eils R and Konig R. Analyzing the regulation of metabolic pathways in human breast cancer. BMC Med Genomics 2010; 3: 39.
[51] Allegra CJ, Hoang K, Yeh GC, Drake JC and Baram J. Evidence for direct inhibition of de novo purine synthesis in human MCF-7 breast cells as a principal mode of metabolic inhibition by methotrexate. J Biol Chem 1987; 262: 13520-13526.
[52] Cao S, Wang L, Zhang Z, Chen F, Wu Q and Li L. Sulforaphane-induced metabolomic responses with epigenetic changes in estrogen receptor positive breast cancer cells. FEBS Open Bio 2018; 8: 2022-2034.

Supplementary Materials and Methods

Gas chromatography-mass spectrometry (GC/MS)

The derivatized samples were analysed on an Agilent 7890B/5977A GC-MS system with a DB-5MS capillary column (30 m × 0.25 mm × 0.25 μm, Agilent J&W Scientific, Folsom, CA, USA). Helium was used as the carrier gas with a constant flow rate of 1 ml/min. The temperature programme was as follows: the initial temperature was held at 60°C for 0.5 min, elevated to 125°C at a rate of 8°C/min, elevated to 210°C at a rate of 4°C/min, and elevated to 305°C at a rate of 10°C/min and maintained for 6 min. The temperatures of the ion source and quadrupole were set to 230°C and 150°C, respectively. The mass range (50-500 m/z) in full-scan mode and electron impact ionization (70 eV) was applied, and the solvent delay time was set to 5 min. The target compound mass spectrometry parameters are shown in Table S1.

Ultra-high-performance liquid chromatography-tandem mass spectrometry method with electrospray ionization (UHPLC-ESI-MS/MS)

The LC system used was an ultra-high-performance liquid chromatograph (Thermo Fisher Scientific, USA) with an Acquity UPLC HSS T3 column (100 mm × 2.1 mm, 1.8 μm) (Waters, Milford, MA, USA). Mobile phases of 0.1% formic acid in water (A) and 0.1% formic acid in acetonitrile (B) were used, and chromatographic separation was performed using the following gradient: 0 min, 100% A; 2.5 min, 100% A; 6.5 min, 65% A; 10 min, 20% A; 11 min, 5% A; 12 min, 5% A; 12.1 min, 100% A and 18 min, 100% A. The flow rate was 0.3 ml min^{-1}, and the injection volume was 5 μl. The MS system used was a TSQ Altis triple quadrupole mass spectrometer (Acquity, Waters, USA) coupled with an electrospray (ESI) ion source and Xcalibur4.0 workstation. The optimized MS conditions were as follows: positive ion spray voltage, 3500 V; anion spray voltage, 2500 V; and ion transfer tube temperature, 325°C. The target compound mass spectrometry parameters are shown in Tables S2 and S3.

Table S1. Information on standard samples in GC/MS

Empirical Formula (Hill Notation)	Abbreviation	CAS Number	Empirical Formula	Molecular Weight
Hypoxanthine	HYP	68-94-0	$C_5H_4N_4O$	136.11
Xanthine	XAN	69-89-6	$C_5H_4N_4O_2$	152.11

Table S2. The information of standard samples in UHPLC-ESI-MS/MS

Empirical Formula (Hill Notation)	Abbreviation	CAS Number	Empirical Formula	Molecular Weight
Inosine	Ino	58-63-9	$C_{10}H_{12}N_4O_5$	268.08
Adenine	A	73-24-5	$C_5H_5N_5$	135.13
5-hydroxyisourate	5-HIU	6960-30-1	$C_5H_4N_4O_4$	184.10966
Uridine 5'-diphosphate	UDP	58-98-0	$C_9H_{14}N_2O_{12}P_2$	404.1612
CDP	CDP	63-38-7	$C_9H_{15}N_3O_{11}P_2$	403.1764
Pseudouridine	ψ	1445-07-4	$C_9H_{12}N_2O_6$	244.2014

Table S3. Mass spectrometry parameters

Empirical Formula (Hill Notation)	Ion mode	Precursor ion (m/z)	Product ion (m/z)
Inosine	-	267	134.97
Adenine	+	268	136.071
5-hydroxyisourate	+	185	--
Uridine 5'-diphosphate	+	402.9	79
CDP	+	401.9	79
Pseudouridine	+	245	179

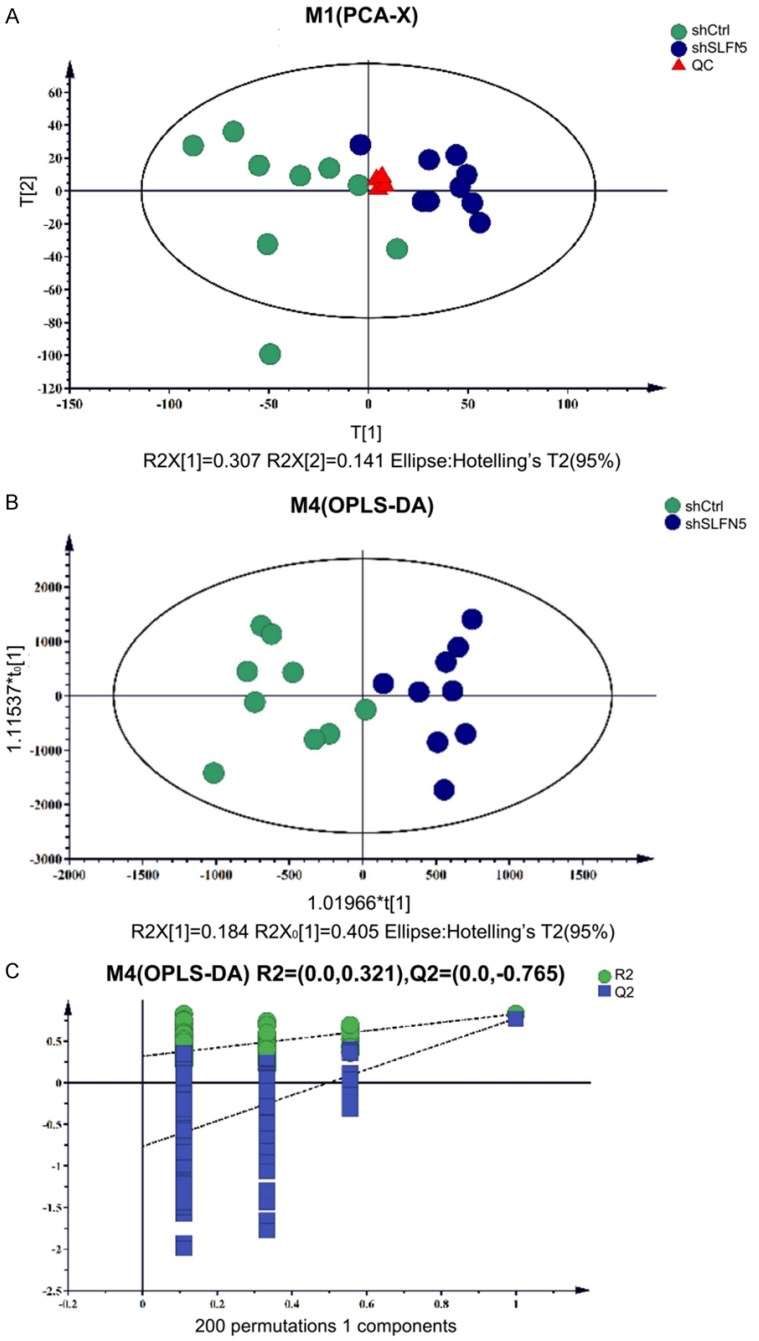

Figure S1. A. PCA score plots based on all samples, including QCs. B. OPLS-DA score plots based on the SLFN5 interference group and control group. C. Statistical validation of the corresponding OPLS-DA model by 7-fold cross validation and RPT (200 times) analysis.